J Mater Sci (2008) 43:3674–3682
DOI 10.1007/s10853-008-2589-y

Coarsening kinetics of metastable nanoprecipitates in a Fe–Ni–Al alloy

M. A. Muñoz-Morris · N. Calderon · D. G. Morris

Received: 22 January 2008 / Accepted: 10 March 2008 / Published online: 4 April 2008

Abstract Microstructure evolution of a Fe–Ni–Al alloy has been examined during annealing at temperatures between about 700 and 800 °C. This material is brittle in the cast state but shows good strength with ductility after a stabilising anneal at 1100 °C when it has a duplex microstructure of B2 dendrites with fcc interdendritic phase. The 700–800 °C ageing leads to the formation of metastable bcc precipitates within the dendrites with less change within the interdendritic regions. The long-term coarsening of these precipitates is controlled by diffusion within the B2 phase. The composition of the B2 phase changes with annealing temperature, which is believed to modify the diffusion rate and, correspondingly, the rate of particle coarsening. The present coarsening study serves to define annealing conditions for preparation of optimum microstructure before material testing, as well as define upper temperature limits for possible long-term application, where stable microstructures are required.

Introduction

Fe–Ni–Al alloys with duplex microstructure composed of B2 ordered phase (essentially NiAl, here called β' phase) and disordered fcc phase (essentially Fe, here called γ phase) are of interest since they may offer a combination of sufficient room temperature ductility to be manageable as engineering materials, good creep resistance (when alloyed with additional strengthening elements) at temperatures above 600–700 °C, and where the high Al content (possibly also with Cr additions) gives good oxidation/corrosion resistance [1–6]. Such alloys cover a range of compositions of 20–60%Fe, 30–50%Ni and 10–30%Al (atomic percent is used throughout) [7]. Other studies with a wider range of Fe–Ni–Al compositions, where a majority β' phase is combined with either α phase (disordered bcc Fe) or with γ' phase ($L1_2$ ordered Ni_3Al) have confirmed that the poor ductility of the majority β' phase is not significantly alleviated [2, 5, 8, 9]. Thermomechanical processing of these alloys has been shown to lead to refinement of the microstructures of these cast B2 or B2 + γ materials, and to produce considerable improvements of the ductility [1–5].

The present study examines the thermal stability of an alloy of composition $Fe_{45}Ni_{35}Al_{20}$ prepared by casting [10]. The Al content of this alloy ensures that the primary β' dendrites are surrounded by a large volume fraction of γ phase, as may be understood by examination of the relevant ternary diagrams, some of which are shown in Fig. 1. The material obtained is relatively strong but has limited ductility. Annealing at high temperature, however, leads to chemical homogenisation and to some coarsening of the duplex microstructure, leading to some softening but to considerable improvements of ductility [10]. As discussed elsewhere [10], the relatively low Ni content was chosen both to achieve relatively low material costs and also to ensure that neither the α Fe phase nor the γ' Ni_3Al phase should form during prolonged exposure at temperatures of around 700 °C, the range of possible engineering interest. The α phase would have low concentrations of both Al and Ni [7], which could be expected to deteriorate oxidation/corrosion behaviour, while the γ' phase does not appear to ensure good overall ductility.

Previous studies [10] have examined the as-cast microstructure of the $Fe_{45}Ni_{35}Al_{20}$ alloy, as well as the changes

M. A. Muñoz-Morris (✉) · N. Calderon · D. G. Morris
Department of Physical Metallurgy, CENIM-CSIC, Avenida Gregorio del Amo 8, Madrid 28040, Spain
e-mail: mmunoz@cenim.csic.es

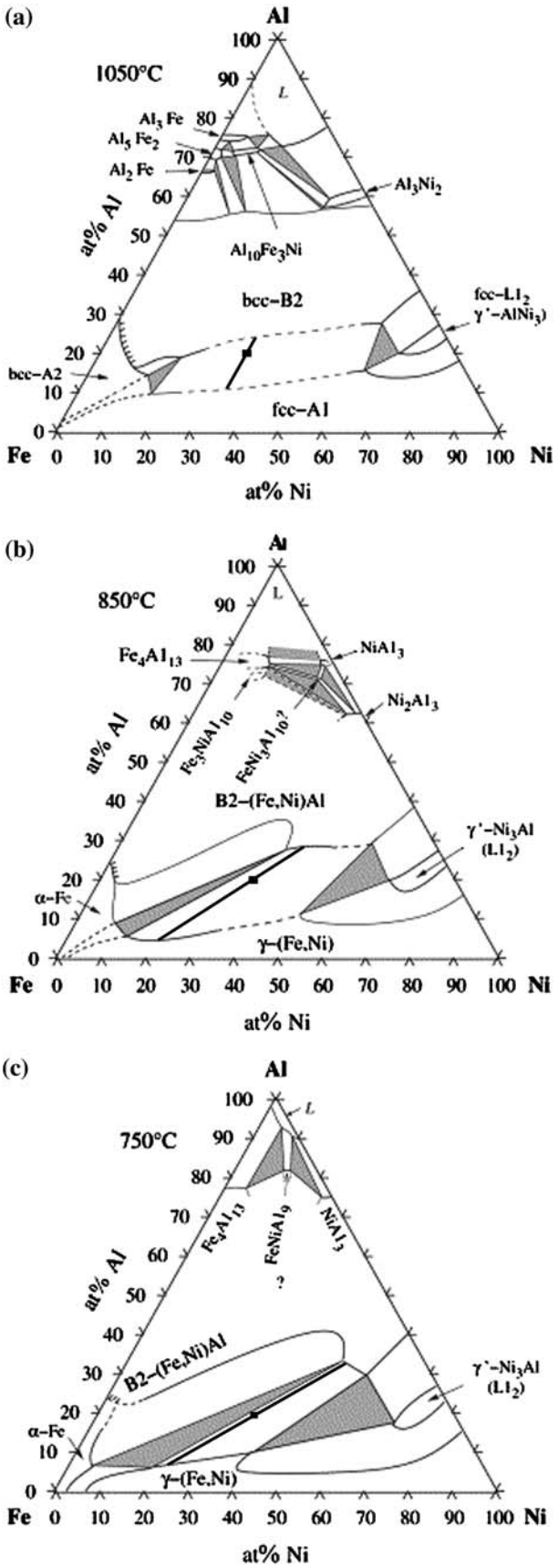

◀ **Fig. 1** Ternary phase diagram sections showing equilibrium compositions at 1050, 850 and 750 °C. Alloy composition (black square) and approximate tie-lines indicating equilibrium β' and γ compositions are shown. Below 1050 °C, big changes of composition of both β' and γ occur, leading to extensive precipitation. Between 850 and 750 °C, there is significant change in the β' composition

occurring during anneals at 1000–1100 °C used to improve ductility. The cast material contains primary β' dendrites, which are chemically inhomogeneous with lower Ni and Al contents at their interior, separated by a γ phase region [10]. After high-temperature annealing the material retains the duplex microstructure of β' dendrites with approximately 25% by volume of γ phase between the dendrites, but now coarse needle precipitates of γ phase are found inside the β' dendrites, and coarse needle precipitates of β' phase found within the γ phase [10]. This microstructure is produced as the as-solidified dendrites and interdendritic phase adjust their compositions to equilibrium at the annealing temperature, indicated in Fig. 1a, and is the state that ensures good room temperature strength and ductility. The relevant chemical compositions of the phases present at these various stages are summarised in Table 1. Further changes of phase composition [7] and microstructure will be expected during exposure at temperatures in the 700–900 °C range, and which may lead to additional changes of mechanical properties. The present study examines microstructural changes occurring during such intermediate temperature annealing, and is useful for two reasons: (i) it can define suitable time–temperature conditions for achieving an appropriate distribution of precipitate particles for obtaining the desired mechanical properties—these might be fine particles (5–20 nm) for highest strength or coarser particles for balanced strength with retention of good ductility; (ii) it can define an upper temperature limit above which material remains unstable and microstructure coarsens at a notable rate, and which can be regarded as an upper temperature for possible long-term applications.

Experimental methods

The alloy studied, of nominal composition 45%Fe–35%Ni–20%Al (atomic percent throughout) was prepared by induction melting, from pure elements, in an Al_2O_3 crucible under argon atmosphere [10]. Solidification took place relatively quickly due to fast heat extraction from the small sample size, giving rise to a segregated, columnar-grain microstructure with moderate dendrite arm spacing of the order of 50 μm. Following casting, this material was given an anneal of 1 h at 1100 °C, followed by water quench. Such a treatment had previously been shown to lead to significant improvements in ductility with retention

Table 1 Chemical compositions of phases present at various stages, as determined by EDS in the SEM or the TEM, or as determined from equilibrium phase diagrams, such as the sections illustrated in Fig. 1

Composition of the microstructural component for the given material state	Fe (at.%)	Ni (at.%)	Al (at.%)
Alloy composition	45	35	20
As cast β' dendrites (core → outside values) [10]	44 → 35	35 → 39	21 → 26
As cast interdendritic film of γ phase [10]	57	31	12
β' phase stabilised at 1050 °C (based on Fig. 1a)	41	35	24
γ phase stabilised at 1050 °C (based on Fig. 1a)	54	35	11
β' phase stabilised at 1100 °C: SEM-EDS	37.0 ± 2	38.2 ± 1	24.8 ± 1
γ phase stabilised at 1100 °C: SEM-EDS	55.9 ± 1	34.1 ± 1	10.0 ± 0.5
β' phase annealed at 850 → 750 °C (Fig. 1b, c)	30 → 18	41 → 49	29 → 33
Change of β' phase composition 1050–750 °C	−23	+14	+9
γ phase annealed at 850 → 750 °C (from Fig. 1b, c)	75 → 71	20 → 22	5 → 7
Change of γ phase composition 1050–750 °C	+17	−13	−4
β' phase stabilised at 800 → 725 °C: SEM-EDS	27.1 → 19.0	42.2 → 48.2	30.6 → 32.8
β' phase stabilised at 800 → 725 °C: TEM-EDS	29 → 21	44 → 50	27 → 29
γ phase stabilised at 800 → 725 °C: SEM-EDS	66.9 → 63.6	26.4 → 28.5	6.7 → 7.9
Precipitates in β' phase, 800 → 725 °C: TEM-EDS	77 → 71	18 → 23	5.5 → 6

Experimental compositions are considered to be correct to within about ±2–5% relative error, i.e. about ±0.5–2% absolute values. β' phase is B2 ordered (Fe, Ni)Al, and γ phase is disordered fcc (Fe, Ni)

of high material strength [10]. Subsequent anneals were carried out in the temperature range approximately 700–800 °C and structural changes examined.

Microstructural changes were documented by both Scanning Electron Microscopy (SEM) using a JEOL 6500F instrument, and Transmission Electron Microscopy (TEM) using a JEOL 2010FX instrument, on thin foil samples prepared using twin-jet electropolishing procedures (details are given elsewhere [10]). The chemical compositions of the β' phase dendritic regions and the γ phase regions, both interdendritic regions and precipitates, were determined by Energy Dispersive Spectroscopy (EDS) analyses both by SEM and by TEM. EDS measurements by SEM used a windowless detector with Ni standard and total analysed composition normalised to 100%. Point analysis was carried out for 100 s count time, and showed an error of ±0.5–2% absolute value of composition depending on the case, corresponding to 2–6% relative value. The same method was used to confirm overall alloy composition to relatively good precision (± 0.5% for each element) by rastering the beam, at low magnification, over a large area (≈ 1 mm^2). EDS measurements in the TEM used an ultrathin detector window, and a standardless analysis was made using the usual thin foil corrections. Spot sizes of 5–30 nm were used, depending on the material analysed, giving count rates near 1,000 counts per second, with a counting time of 100 s. Analyses were carried out on thin sample regions (50–100 nm depending on the fineness of the microstructure), with the sample tilted 10° towards the detector. Experience has shown that results vary with sample thickness and tilt; nevertheless, good precision can be expected when comparing medium/heavy elements (e.g. Fe, Ni), but light elements (e.g. Al) have been found to be underestimated by up to 10% (relative error). In the following work, phase compositions determined by TEM-EDS can only be taken as indicative with regards the Al content, but the Fe/Ni ratio can be expected to be reliable. For all cases, phase compositions reported are the average of about 10 measurements made for each region of a given material without changing microscope or sample configurations.

Experimental results

Mechanical property changes

The present study concentrates on changes of microstructure occurring in the cast-stabilised material with the intention of determining ageing conditions whereby stable particles are produced which can achieve useful high-temperature creep strengthening. In particular, since the present materials show limited but not outstanding ductility, and since prior studies on similar materials [3] have shown that ageing to maximum hardening also leads to material embrittlement, no attempt has been made to study such age rehardened materials. In this previous study [3], significant hardening and embrittlement was found for annealing treatments which led to the appearance of precipitates of size 5–10 nm, while such hardening was lost

Table 2 Mechanical properties determined by tensile testing on material in various heat-treated states

Material state	Yield stress (MPa)	Maximum/Fracture stress (MPa)	Tensile elongation (%)
As cast	930	930	$\approx$0.1
Annealed 1 h at 1000 °C	810	890	0.6
Annealed 1 h at 1100 °C	600	990	3

All tests were carried out at room temperature using a nominal strain rate of 2×10^{-4}/s

and material reductilised when overageing led to particles of size near 50 nm. The present study accordingly has concentrated on those ageing treatments that produced similarly coarse precipitates, which will be somewhat more stable against further coarsening, but which can nevertheless be expected to produce some high-temperature strengthening. Creep testing underway, to be reported at a later date, shows that materials containing a high density of coarse precipitate particles, of size near 100 nm, indeed show significant improvements of creep resistance at temperatures of near 700 °C.

Results of tensile testing on samples machined from the cast and annealed materials are given in Table 2. As mentioned above, the as-cast material is strong but brittle, while annealing at temperatures of 1000–1100 °C leads to considerable softening and the onset of small amounts of ductility. In particular, the material annealed at 1100 °C shows sufficient ductility for easy handling as an engineering material, and was selected as that for subsequent ageing studies.

Microstructural changes during heat treatments

The as-cast material has a duplex microstructure comprising β' dendrites and interdendritic γ phase [10]. The chemical composition of the alloy determined by SEM-EDS is identical, within the $\pm$0.5% error, to the nominal composition shown in Table 1. Following the stabilising anneal at 1000–1100 °C, which ensures that the overall ductility is reasonable, the material still shows the same β' dendrites–γ interdentritic region microstructure. In addition, however, the β' dendrites now contain coarse needles of the γ phase, and the interdendritic γ phase now contains coarse needles of β' phase, as shown in Fig. 2. Figure 2a shows the duplex dendrite–interdendrite microstructure, with the coarse needle precipitates inside both the dendrites and the interdendritic region. Figure 2b shows details of the needle precipitates at higher magnification, with the γ phase regions (both interdendritic region and in-dendrite needles) showing also finer secondary decomposition. The chemical compositions of the β' phase and the γ phase regions, both the dendrite/interdendrite regions and the coarse needle precipitates, as determined by EDS, are in good agreement with expected equilibrium compositions for the two phases at these high temperatures [7, 10] (see Table 1). Table 1 shows the expected equilibrium compositions for both β' and γ phases in equilibrium at 1050 °C [7], for comparison with experimental values measured on material annealed at 1100 °C. It should be noted that almost identical compositions are expected for equilibrium at both 1050 and 1150 °C [7]. Comparison with the expected values in Table 1 shows that the experimental values have, for β' phase, a slightly lower Fe content and slightly higher Ni content, while for the γ phase there is a slightly higher Fe content and lower Ni content—in neither case dramatically different from phase diagram expectations.

Following further lower-temperature annealing, in the range 700–800 °C, fine precipitation occurs inside the β' phase dendrites, with no obvious new precipitation inside the γ phase regions (see Fig. 2c). Such precipitation can be understood by examination of the ternary phase diagram [7] (Fig. 1), where it is clear that on lowering the temperature from near 1100 to 750 °C the composition of the β' phase changes greatly, with a smaller, albeit significant, change occurring also in the γ phase region. These phase compositions and the change of composition are also summarised in Table 1. The change of composition in the β' phase region is accomplished by the precipitation of fine particles of what is expected to be γ phase (see Fig. 1b, c) with the interparticle separation being much smaller than the size of the β' phase regions between the coarse particles (see Fig. 2c). Equivalent precipitation of β' phase particles would be expected within the γ phase regions (both the interdendritic γ region and the coarse γ needles). However, no precipitation is detected within these γ phase regions, presumably because these regions are fine and contain many interfaces (see Fig. 2c). It is possible that the matrix composition change can be accomplished by solute deposition at these interfaces. Experimental measurements of chemical composition by SEM-EDS (Table 1) confirm a β' phase composition very close to that expected after 800–725 °C annealing, and a γ phase composition slightly low in Fe and rich in Ni. The SEM measurements of chemical composition of the β' phase were made in the precipitate-free zones surrounding these regions after the low temperature anneals (see Fig. 2c) to avoid simultaneous measurement of the β' matrix and the precipitates.

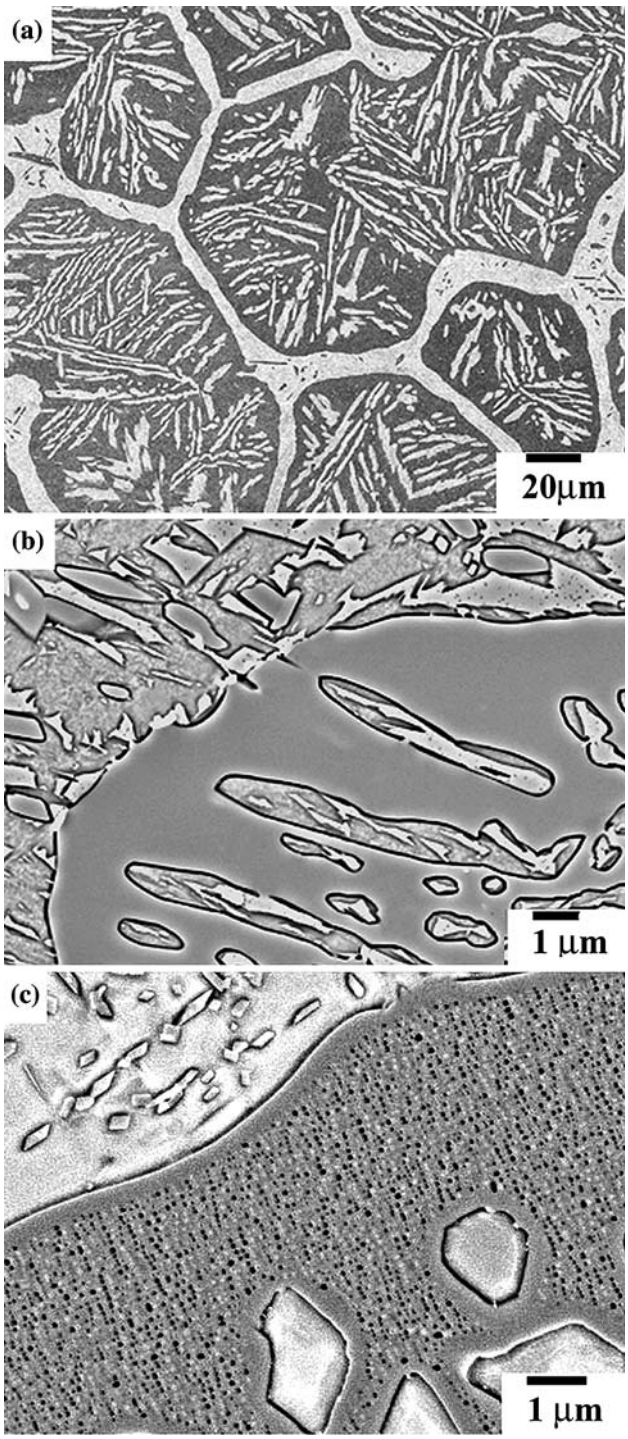

Fig. 2 (**a**) and (**b**) As-cast microstructure after the 1 h–1100 °C stabilisation anneal; (**c**) fine precipitation inside β' dendrites on further annealing 36 h at 750 °C. SEM images using back-scattered electron contrast

Determination of chemical composition by TEM-EDS (Table 1) shows slightly higher values for Fe and Ni content for the β' phase with slightly lower levels of Al. Examination of the fine precipitates inside the β' phase regions showed that these had somewhat higher levels of Fe but lower levels of Ni and Al than measured by SEM-EDS in the γ phase regions. These measured TEM-EDS values remain, nevertheless, similar to compositions expected for equilibrium γ phase at 800–725 °C (see Table 1).

Similar precipitates have been observed previously [3, 6] and shown to produce significant age hardening when the precipitates are fine [3], but not to improve ductility [3, 6]. The precipitates were identified there as α phase, as expected in alloys with equal Ni and Al contents [6, 7], and also in alloys with higher Ni or Al contents at very low annealing temperatures [3]. It is important to determine the composition and structure of the precipitates seen here, as well as the temperature range where they can be retained without excessive coarsening.

Figure 3 shows examples of precipitates, similar to those of Fig. 2c, found inside the β' dendrites of materials aged at 725–775 °C for various times. Precipitates were seen as rounded cuboids, homogeneously distributed throughout the dendrites apart from a thin precipitate-free zone near the dendrite-γ region, as seen in Fig. 2c. At long annealing times some coalescence of precipitates into slightly elongated rods was observed (see Fig. 3d) similar to the rafting phenomenon observed in γ–γ' superalloys [11].

Examination of these precipitates by TEM using a large selecting area aperture found no additional diffraction spots over those corresponding to the β' matrix. Greatly weakened superlattice spots, nearly disappearing, were observed when using a small selected area aperture over a single precipitate particle. Dark field imaging using a superlattice spot of the B2 ordered matrix showed dark precipitates in the light matrix (see Fig. 4a). Furthermore, little contrast change was seen between matrix and precipitates in both bright field and dark field images when using fundamental imaging vectors (see Fig. 4b). These observations confirm that the precipitate (a) does not have a completely different structure or orientation from the matrix; (b) has an extremely low level of order, or is completely disordered bcc structure. It is clearly α phase and not γ phase, as is expected from the ternary phase diagram [7]. The chemical analysis by TEM-EDS (Table 1) confirmed that these fine precipitates had a low Al content, about 5–6%, and a Ni content of 20 ± 2%. Examination of the ternary phase diagram (Fig. 1c) for the 800–725 °C ageing temperatures shows that the β' phase is expected to be in equilibrium with γ phase having similar composition to this (Fe–20%Ni–5%Al: Fig. 1b, c), while the α phase is expected to have a much lower Ni content (Fe–8%Ni–8%Al: Fig. 1b, c). These α precipitates are clearly metastable in the β' matrix.

Precipitate sizes have been determined from micrographs such as those of Fig. 3, analysing 800–1,000

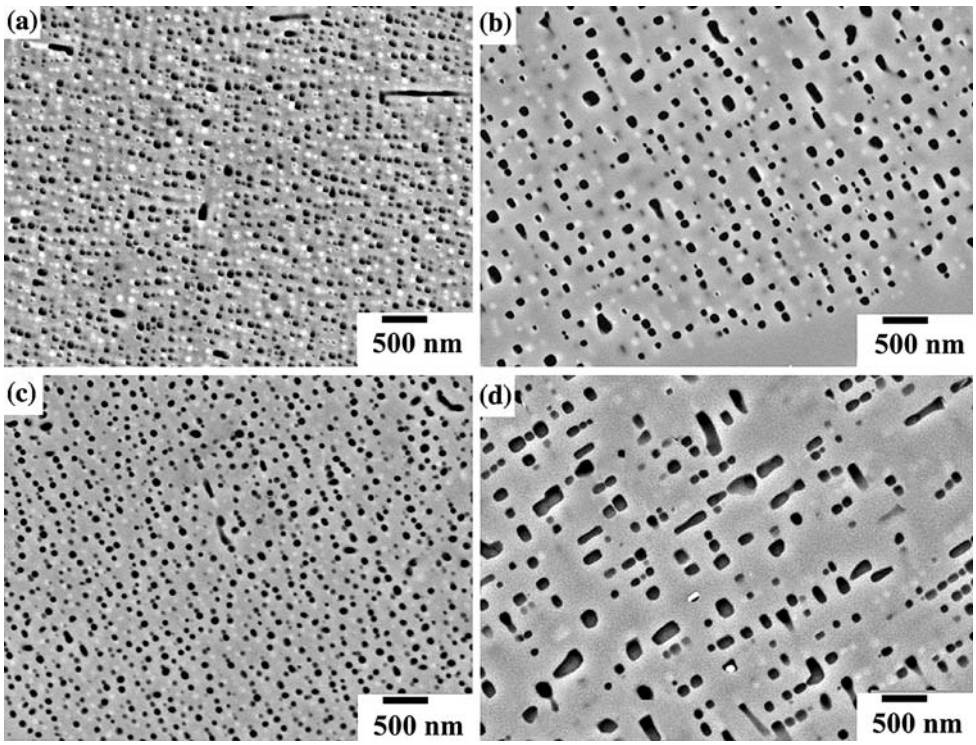

Fig. 3 Fine precipitates formed on ageing the cast-stabilised material for: (**a**) 48 h at 725 °C; (**b**) 120 h at 725 °C; (**c**) 6 h at 775 °C; and (**d**) 48 h at 775 °C. SEM images using back-scattered electron contrast

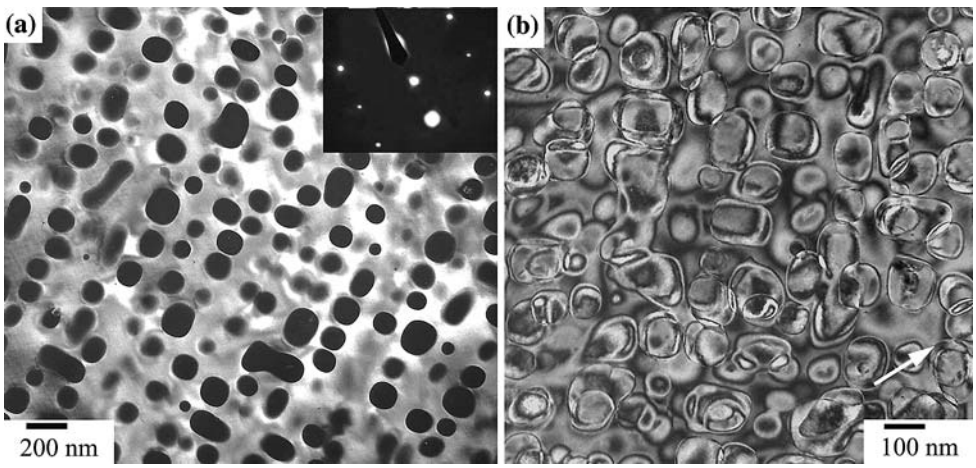

Fig. 4 Dark field TEM images showing: (**a**) low intensity of precipitates when imaging using a 001 beam of the B2 matrix; diffraction pattern (inset) taken using a large selecting aperture showing spots corresponding to ⟨110⟩ B2 zone axis; (**b**) similar contrast of precipitates in β' matrix. Imaging 110 **g** vector is shown arrowed. Material aged for 48 h at 750 °C

particles for each state. Histograms of particle size distributions are illustrated in Fig. 5, from which average sizes have been determined, as shown in Fig. 6. Over the range of annealing conditions examined the particle sizes varied from below 50 nm to above 150 nm. Shorter annealing times have not been considered because the associated smaller precipitates are expected to embrittle the material even though they produce greater strengthening. The range of annealing times shown in Fig. 6 extends roughly to that before the onset of rafting, where the particle size can be well represented by the diameter of the circular particle of equivalent area.

Discussion and conclusions

The Fe–Ni–Al alloy examined here has a composition that leads to a duplex microstructure after casting, which is strong but shows only limited ductility. The duplex dendrite/interdendrite phase microstructure is softened by anneals above about 1000 °C leading to improvements in ductility to several percent elongation. These anneals lead to β' dendrite and γ interdendrite phases in equilibrium at the high temperature, with coarse needle precipitates within both phase regions. Subsequent anneals at intermediate temperatures (700–800 °C) lead to precipitation of

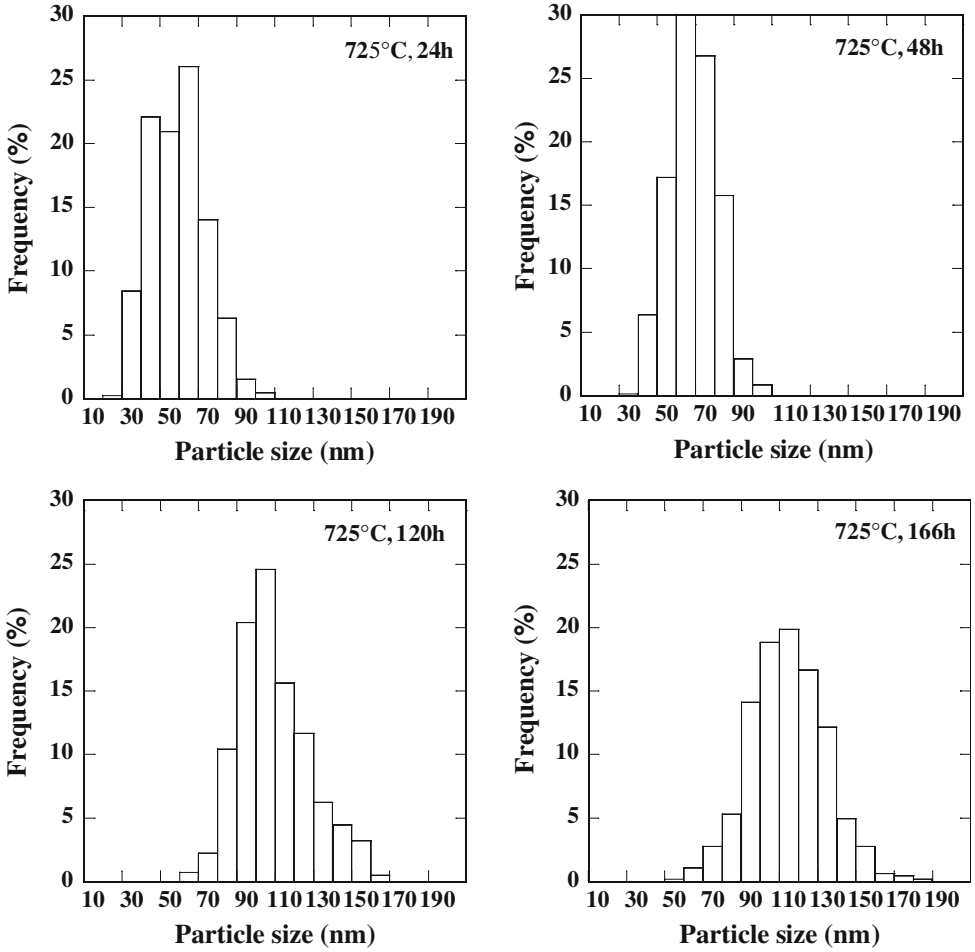

Fig. 5 Histograms showing frequency of particle sizes after various annealing treatments

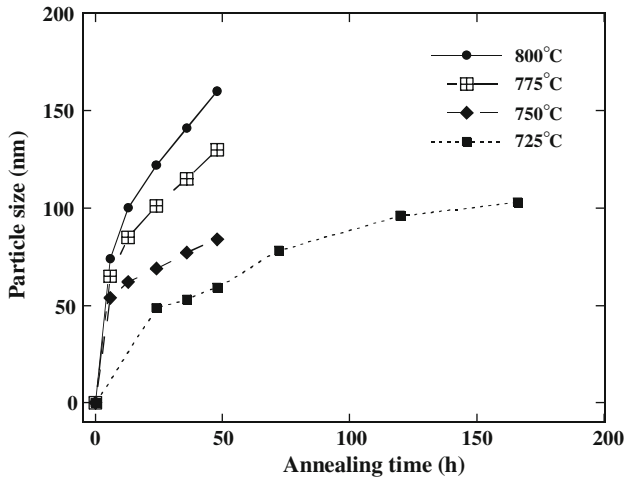

Fig. 6 Increase of particle size on annealing at temperatures in the range 725–800 °C

fine particles within the β' dendrites (see Fig. 2) as the equilibrium composition of the phase changes (Fig. 1). A corresponding change in the equilibrium composition of the γ phase (Fig. 1) does not lead to additional precipitation within this phase region in view of the high density of particles and interfaces (see Fig. 2) which provide many sinks for accommodation of composition changes.

The present study set out to determine the annealing conditions which lead to precipitation and coarsening of these precipitates within the β' dendrites. It has been shown previously [3, 6] that similar precipitates can produce significant room temperature strengthening when present as fine ($\approx$5–10 nm) particles, but which can also embrittle this only just-sufficiently ductile material. Nevertheless, the presence of a high density of coarser ($\approx$50–100 nm) particles can be expected to produce useful high temperature strengthening under slow strain, creep conditions. A quick estimate of the Orowan strengthening produced by such particles gives values of the order of 100 MPa, and preliminary creep testing indeed shows particle strengthening of similar magnitudes (data to be reported at a later date). It is thus of interest to know what ageing times and temperatures are required for obtaining such suitably sized precipitate particles. The study of particle coarsening rate (Fig. 6) confirms that anneals of several hours at temperatures below 800 °C are suitable for obtaining the desired particle sizes. The same study confirms that the precipitate particles will remain smaller than about 100 nm for moderate times at a

temperature of 725 °C (Fig. 6). Such a material, with 100 nm precipitate particles, will be expected to be stable against further significant coarsening for extremely long times at temperatures of about 650 °C, and this can then be seen as an upper temperature limit for long-term high-temperature operation of materials based on the present alloy.

The composition of the β' phase present in the $Fe_{45}Ni_{35}Al_{20}$ alloy, and its change from the initial 1100 °C anneal to the 725–800 °C ageing temperatures, has been shown in Fig. 1 and Table 1. Note that the composition of the β' phase hardly changes between temperatures of 1050 and 1150 °C [7], and hence the 1050 °C isotherm shown in Fig. 1a is a good approximation of the compositions expected for the 1100 °C anneal used. On lowering the temperature from 1100 to 800–725 °C the equilibrium composition of the β' matrix phase changes dramatically, as illustrated in the isotherms of Fig. 1b, c and reported in Table 1. The experimentally determined compositions of the β' dendrites and the coarse γ phase regions are in excellent agreement with the published phase diagrams (noting that the available low-temperature isotherms correspond only approximately to the range of annealing temperatures examined). On the basis of these equilibrium isotherms, the change of composition of the β' phase dendrite matrix is expected to lead to the appearance of γ phase precipitates, not the α phase precipitates identified. The crystallographic nature of this precipitate phase has been clearly identified by the weak/absent superlattice spots in diffraction patterns, confirming the disordered bcc structure, not the ordered B2 structure of the matrix, and by the dark field images obtained using superlattice B2 reflections of the matrix (Fig. 4a). The chemical composition of these precipitates, as determined in the TEM, is clearly subject to considerable uncertainty, but the composition determined corresponds very approximately to that expected of γ phase and is far from that expected of α phase. As such, the precipitates formed are considered to adopt the metastable α phase structure and not the equilibrium γ phase structure.

Examination of equilibrium diagram isotherms near the relevant 725–800 °C temperature range (Fig. 1b, c) shows that the alloy investigated ($Fe_{45}Ni_{35}Al_{20}$) has a composition close to the three-phase β'–γ–α region, and indeed some α phase precipitates were observed in a previous study of the same alloy [10] when ageing the inhomogeneous, as-cast alloy at a temperature of 750 °C. Indeed one possible reason for the formation of precipitates of α phase instead of the expected γ phase might be an error of overall alloy composition. Experimental analysis of the bulk alloy by EDS has confirmed the chemical composition to be that expected but this method of analysis is subject to some uncertainty. Examination of the phase diagram isotherms (Fig. 1b, c) shows that the β' phase regions must be impoverished in Ni by about 3%, with the Al content perhaps increasing by about

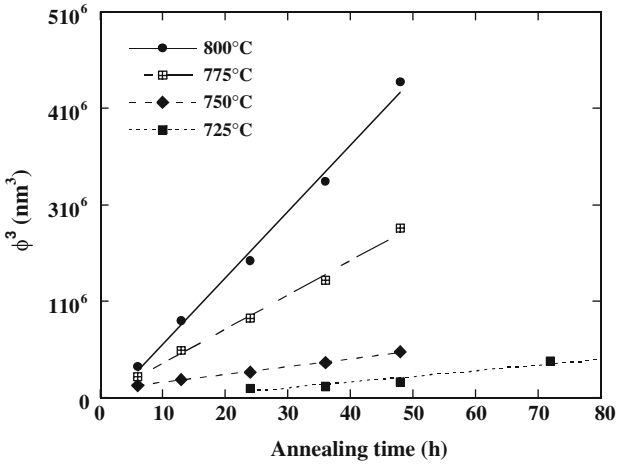

Fig. 7 Coarsening rate of particles on annealing represented as a size (ϕ) cubed–time relationship

1%, in order to avoid completely the formation of mixed α and γ precipitate phases on annealing at 725–800 °C. Such a discrepancy of bulk alloy composition, especially with regards the Fe/Ni ratio, seems unlikely. As such, the metastable nature of the α phase precipitates is confirmed.

The appearance of metastable states is not uncommon during the early stages of precipitation in many metallic systems. It is, however, somewhat more unusual for such metastability to be retained to such large particle sizes and for long annealing treatments. Examination of the ternary isotherms for the relevant β' matrix composition (Fig. 1b, c) shows that the expected β' and γ phase compositions lie very close to the edge of the three-phase β'–γ–α region. As such, the α phase may be considered as being only marginally thermodynamically unstable, with the lower energy for the β'–α interface relative to that of the β'–γ interface leading to an overall preference for particles of the α phase up to relatively large particle sizes.

The particle size data shown in Fig. 6 can be very well described by a size cubed–time relationship, passing very close to the size-time origin (Fig. 7). The observation that these lines pass through the origin confirms that precipitation processes finished at very short times for these temperatures, and subsequent particle growth took place by coarsening alone [12].

The slope of the size cubed–time line in Fig. 7 is dependent on the solubility (C) of the controlling species (in the β' matrix), the diffusivity (D) of this solute, as well as the precipitate–matrix interface energy (σ), and can be written [12]:

$$\phi^3 - \phi_0^3 = \frac{64C\sigma DV_m}{9RT}t \quad (1)$$

where ϕ and ϕ_0 are the particle size after annealing and before annealing, respectively, V_m is the molar volume of the precipitate material, and t, R, and T are the annealing

time, the gas constant, and the annealing temperature, respectively. The temperature dependence of this slope has been shown to obey the Arrhenius law, with an activation energy of 325 kJ/mol. This value may be related to the temperature changes of solubility and diffusivity. Studies of diffusivity of Ni and Al in the ternary Fe–Ni–Al β' phase [13] have, however, determined an activation energy for diffusion of 275 kJ/mol, significantly lower than the value deduced from the present coarsening data.

Two possible explanations may be proposed for the difference between these two values of activation energy. Examination of the ternary phase diagrams as temperature changes [7] (Fig. 1) shows that there are significant changes of Fe, Ni and Al contents as the α phase precipitates out in the β' phase matrix, and the composition of the β' phase itself changes significantly depending on the ageing temperature. As such, the value of C in Eq. 1 is itself temperature dependent. Expressing this composition change in terms of thermally activated solubility in an ideal solution, an activation energy of 30 $\pm$15 kJ/mol is deduced (the uncertainty arises because it is not clear whether the composition change of Fe, Ni or Al should be considered). Alternatively, it may be the change of composition of the β' phase that leads to a change of the diffusivity controlling coarsening. It is the composition of the β' phase matrix in the 725–800 °C temperature range that is important for determining the coarsening rate, and this composition changes significantly with ageing temperature (Table 1). It is, for example, known that adding Fe into the binary β' NiAl compound lowers the diffusivity [13–15], with a diffusivity minimum occurring near 10%Fe. Extensive work on the influence of chemical composition on diffusivity in Fe–Ni–Al alloys has been carried out at high temperatures [16–18], and can be used to examine likely composition effects on diffusivity. These studies [16–18] give diffusion data at 1000 °C for alloys of composition similar to the present one, with diffusion rates shown as dependent on Al content, for a fixed Fe/(Fe + Ni) level of 0.25, or as dependent on Fe/(Fe + Ni) level for a fixed Al content of 30%. For the range of ageing conditions examined here, lowering the ageing temperature leads to a significant drop in Fe content in the β' matrix, with corresponding increases in the Ni and Al contents (see Table 1). As shown in Ref. [18], this change of matrix composition can be expected to give rise to a change of diffusivity, by an additional factor of 2–3. The Al content in the β' matrix for the present alloy is close to 30% and the Fe/(Fe + Ni) level about 0.42–0.27, similar to values for the literature data used in this interpretation. This additional increase in diffusivity by a factor of 2–3 as the matrix Fe content rises and the Al content falls [18] with change of temperature can be described as equivalent to an additional activation energy of about 80 $\pm$ 30 kJ/mol. As such, the high activation energy for coarsening of the α precipitates in the β' matrix may be associated with three factors—diffusivity levels of the controlling species due to thermal activation, change in composition of the matrix and hence concentration of the diffusing species, and change in diffusivity brought about by the change of matrix composition.

The β' phase matrix where α phase precipitation takes place may in fact be disordered during the 1100 °C anneal (this is uncertain), but will certainly be well ordered over the 725–800 °C ageing temperature range, with its Al content near 30% (see Table 1). Nevertheless, ordering kinetics are extremely rapid at these temperatures [19] such that ordering of the possibly disordered β' matrix will take place during the early stages of precipitation, and certainly be completed before the range of coarsening times examined. This comment is important since it is known that the onset of order may affect the rate of diffusion [20], but it is clear that this factor will not have contributed to the coarsening rates that have been determined.

Acknowledgement N. Calderon would like to acknowledge financial support through a M.E.C. pre-doctoral scholarship (FPI–BES–2004–4478).

References

1. Guha S, Munroe P, Baker I (1989) Scripta Metall 23:897. doi:10.1016/0036-9748(89)90267-6
2. Guha S, Munroe PR, Baker I (1991) Mater Sci Eng A 131:27. doi:10.1016/0921-5093(91)90341-J
3. Guha S, Baker I, Munroe PR, Michael JR (1992) Mater Sci Eng A 152:258. doi:10.1016/0921-5093(92)90076-D
4. Guha S, Baker I, Munroe PR (1996) J Mater Sci 31:4055. doi:10.1007/BF00352668
5. Letzig D, Klower J, Sauthoff G (1999) Z Metallkd 90:712
6. Munroe PR, George M, Baker I, Kennedy FE (2002) Mater Sci Eng A 325:1. doi:10.1016/S0921-5093(01)01403-4
7. Eleno L, Frisk K, Schneider A (2006) Intermetallics 14:1276. doi:10.1016/j.intermet.2005.11.021
8. Jung I, Sauthoff G (1989) Z Metallkde 7:484
9. Stallybrass C, Schneider A, Sauthoff G (2005) Intermetallics 13:1263. doi:10.1016/j.intermet.2004.07.048
10. Muñoz-Morris MA, Morris DG (2007) Mater Sci Eng A444:236. doi:10.1016/j.msea.2006.08.082
11. Webster GA, Sullivan CP (1967) J Inst Metals 95:138
12. Porter DA, Easterling KE (1983) Phase transformations in metals and alloys. Van Norstrand Reinhold, Wokingham, UK
13. Divinski S, Kong YS, Löser W, Herzig Ch (2004) Intermetallics 12:511. doi:10.1016/j.intermet.2004.01.003
14. Rudy M, Sauthoff G (1986) Mater Sci Eng 81:525. doi:10.1016/0025-5416(86)90289-2
15. Wang YL, Jones IP, Smallman RE (2006) Intermetallics 14:800. doi:10.1016/j.intermet.2005.12.008
16. Moyer TD, Dayananda MA (1976) Metall Mater Trans 7A:1035
17. Cheng GH, Dayananda MA (1979) Metall Mater Trans 10A:1415
18. Sohn YH, Dayananda MA (2002) Metall Mater Trans 33A: 3375. doi:10.1007/s11661-002-0326-8
19. Lawley A, Cahn RW (1961) J Phys Chem Solids 20:204. doi:10.1016/0022-3697(61)90007-5
20. Sohn YH, Dayananda MA (1999) Scripta Mater 40:79